DECEMBER 1995

ECN-I--95-046

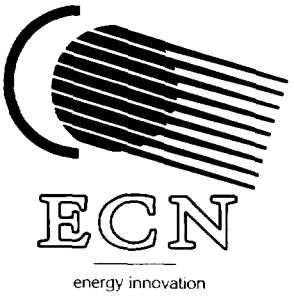

CALCULATION OF FLUENCE RATE DISTRIBUTIONS IN A PRE DESIGN CLINICAL FACILITY FOR BNCT AT THE LFR

T.T.J.M. PEETERS
W.E. FREUDENREICH

The Netherlands Energy Research Foundation ECN is the leading institute in the Netherlands for energy research. ECN carries out basic and applied research in the fields of nuclear energy, fossil fuels, renewable energy sources, policy studies, environmental aspects of energy supply and the development and application of new materials.

ECN employs more than 800 staff. Contracts are obtained from the government and from national and foreign organizations and industries.

ECN's research results are published in a number of report series, each series serving a different public, from contractors to the international scientific world.

The I-series is for internal reports that contain results mainly of interest for (fellow) colleagues, principally within ECN but also for those employed elsewhere. Although these reports may not be in their final form, they may be referred to.

Het Energieonderzoek Centrum Nederland (ECN) is het centrale instituut voor onderzoek op energiegebied in Nederland. ECN verricht fundamenteel en toegepast onderzoek op het gebied van kernenergie, fossiele-energiedragers, duurzame energie, beleidsstudies, milieuaspecten van de energievoorziening en de ontwikkeling en toepassing van nieuwe materialen.

Bij ECN zijn ruim 800 medewerkers werkzaam. De opdrachten worden verkregen van de overheid en van organisaties en industrieën uit binnen- en buitenland.

De resultaten van het ECN-onderzoek worden neergelegd in diverse rapportenseries, bestemd voor verschillende doelgroepen, van opdrachtgevers tot de internationale wetenschappelijke wereld.

De I-serie is de serie interne rapporten die resultaten bevat bestemd voor de ECN-collega's, maar ook voor vakcollega's die elders werkzaam zijn. Deze rapporten hebben een minder definitief karakter, maar zijn wel refereerbaar.

Netherlands Energy Research Foundation ECN
P.O. Box 1
NL-1755 ZG Petten
the Netherlands
Telephone : +31 2246 49 49
Fax : +31 2246 44 80

This report is available on remittance of Dfl. 35 to:
ECN, Facility Services,
Petten, the Netherlands
Postbank account No. 3977703.
Please quote the report number.

Energieonderzoek Centrum Nederland
Postbus 1
1755 ZG Petten
Telefoon : (02246) 49 49
Fax : (02246) 44 80

Dit rapport is te verkrijgen door het overmaken van f 35,-- op girorekening 3977703 ten name van:
ECN, Faciliteiten
te Petten
onder vermelding van het rapportnummer.

DECEMBER 1995

ECN-I--95-046

KS0020419 06
R: FI
DE008847437

DE008847437

CALCULATION OF FLUENCE RATE DISTRIBUTIONS IN A PRE DESIGN CLINICAL FACILITY FOR BNCT AT THE LFR

T.T.J.M. PEETERS
W.E. FREUDENREICH

ECN project 11099.03

Prepared by	: W.E. Freudenreich	Initial :
Position	: Responsible Engineer	
Date	: 13.11.95	
Reviewed by	:J.B.M. de Haas	Initial :
(On behalf of co-readers)		
Position	: Reactor Scientist	
Date	: 13.11.95	
Approved by	: H. Gruppelaar	Initial :
Position	: Head of Group Nuclear Analysis	
Date	: 12-12-95	

Abstract

In a previous study [1], it was demonstrated that the creation of a thermal neutron facility for clinical BNCT in the LFR is feasible. Monte Carlo calculations had shown that the neutron fluence rates and gamma dose rates at the detector position of a model representing a first outline of a clinical facility met all requirements that are necessary for clinical BNCT. In order to gain more information about the neutron fluence rates at several positions, a second step is required. Calculations have been performed for the free beam and for a tumour bearing phantom at 5 cm and 10 cm distance from the irradiation window. Due to thermalization and back scattering, the thermal fluence rates in the tumour at 5 and 10 cm distance from the bismuth shield appeared to be approximately twice as high as the thermal fluence rates in the free beam at the corresponding positions of 5 to 6 cm and 10 to 11 cm from the irradiation window.

Keywords

BNCT
LOW FLUX REACTOR
THERMAL NEUTRON FACILITY
PHANTOM

CONTENTS

1. INTRODUCTION

The primary objective of the Petten BNCT project is focused on the treatment of brain tumours, not curable by conventional therapy but accessible by the two components, a tumour specific boron compound and epithermal neutrons, combined in the binary cancer therapy BNCT. It is expected that clinical trials on glioma-patients by BNCT will start within a few months. The aim of the clinical trials is to verify that BNCT is safe for healthy tissue and efficient in selective destruction of malignant tissue.

There is a strong confidence about a positive demonstration of these unique features of BNCT through the clinical trials. Therefore various investigators worldwide search for further application of BNCT to other tumours than brain tumours. As the therapy reaction $^{10}B(n, \alpha)^{7}Li$ almost exclusively results from capture of thermal neutrons it is evident that a beam of thermal neutrons can be applied with advantage to the treatment of superficial tumours.

In anticipation of increasing demand for additional neutron sources for extended future clinical application of BNCT a feasibility study on a thermal neutron facility at the Argonaut Reactor of ECN, the Low Flux Reactor LFR, has started. A previous investigation [1] has demonstrated that the LFR can provide a neutron beam for clinical application. In this study, a part of the present thermal column was replaced by a moderator, consisting of 0.5 mol % H_2O and 99.5 mol % D_2O. The thickness of this material was 23 cm. The moderator was enclosed by an aluminium tank, its wall thickness being 0.5 cm. A Bismuth slab of 12 cm thickness was placed between the aluminium tank and the irradiation position to shield the gamma rays. Except for a window of 20 x 20 cm^2, the outward surface of this slab was covered by an 0.2 cm thick 100 % enriched ^{6}LiF sheet in order to reduce the unwanted thermal neutron fluence rate outside the irradiation window. Monte Carlo calculations using this model showed that for the neutron fluence rates and gamma dose rates at the detector position (see [1]) all three requirements for clinical BNCT were met:

1. $\phi_{th}/\phi_f = 1700 > 1000$
2. $\phi_{th} / \dot{D}_\gamma = 1.5E+13 > 1.4E+13$ [cm^{-2}/Gy]
3. $\phi_{th} = 1.6E+09 > 1.2E+09$ [$cm^{-2}s^{-1}$]

In order to get more information on the distribution of the neutron field, three more calculations are required: [2]

1. Calculation of neutron fluence rates for the free beam for 4 energy groups: E < 0.5 eV, 0.5 eV < E < 10 keV, 10 keV < E < 1MeV and E > 1MeV.
2. Calculation of neutron fluence rates for the tumour bearing phantom at 5 cm distance from the irradiation window.
3. Calculation of neutron fluence rates for the tumour bearing phantom at 10 cm distance from the irradiation window.

Furthermore,

- The dimensions of the models for the free beam and for the tumour bearing phantom should be large enough to show a decrease of the thermal fluence rate ($E < 0.5$ eV) by a factor of 20 at least.
- All calculations are to be performed with the Monte Carlo code MCNP4A [4], using JEF2.2 cross sections [3].

This report first shows the models that were used for the calculations of the neutron fluence rates in the free beam and in the tumour bearing phantom. Next, for a number of relevant positions in the free beam and the tumour bearing phantom, calculated neutron fluence rates are given.

2. MCNP4A MODEL

2.1 Free beam

The neutron current in the free beam at the centre of the irradiation window is peaked forward, as may be seen in fig. 3.1 of [1]. As there will be relatively few collisions of neutrons in the air behind the bismuth slab, it is assumed that most neutrons will move from the slab in a cone, the top of the cone being located at the centre of the irradiation window and its centerline perpendicular to the bismuth slab. The angle between the surface of the cone and the centre line of the cone roughly amounts to 45 degrees.

Assuming azimuthal symmetry, the cone is discretized into cilinders and each cilinder is divided into rings of equal radial thickness. Fig. 2.1 gives the cells of this MCNP4A model in the direct vicinity of the irradiation window. The total cell structure of the free beam model, together with the bismuth shield, the D_2O moderator slab and part of the reactor is given in fig. 2.2.

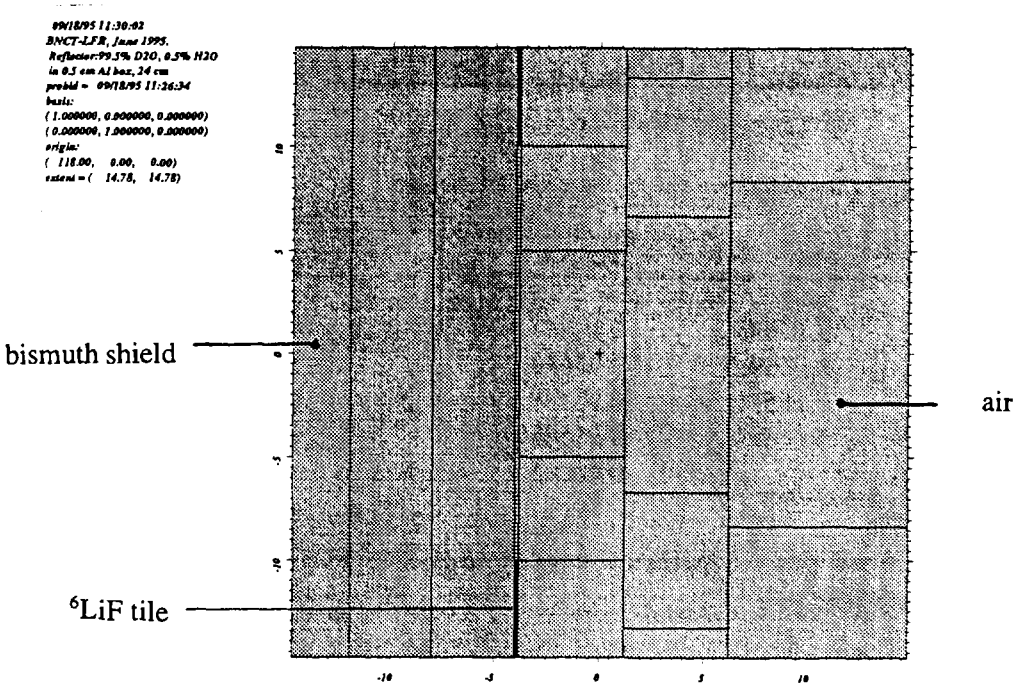

Figure 2.1 Detailed view of cells in the MCNP4A model of the free beam in the direct vicinity of the irradiation window.

2.2 Tumour bearing phantom

The composition of the tissue [5] that was taken for the phantom and the tumour is given in table 2.1

The tumour bearing phantom was given [5] as a 50 x 50 x 20 cm^3 box, filled with tissue material as specified in table 2.1. The tumour is located as a "blister" between a spherical surface of a sphere with a 3.625 cm radius, its origin being located 2.625 cm at the phantom center line inside the phantom, and the surface of the phantom. Compared to the phantom composition, the composition of the tumour contains 30 ppm ^{10}B. The surface of the healthy tissue of the phantom

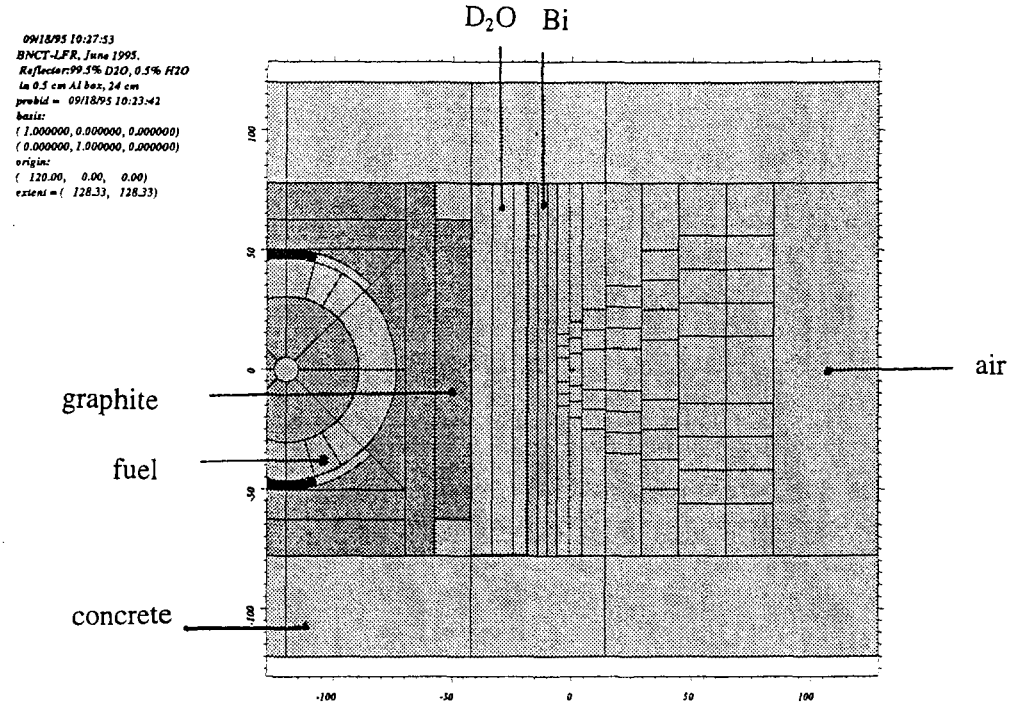

Figure 2.2 Overview of the MCNP4A model of the free beam, the bismuth slab, the D_2O moderator and the reactor.

Table 2.1 *Composition of the phantom and the tumour*

nuclide	phantom	tumour
	weight fraction (ρ = 1.0 gcm^{-3})	
H	0.10095	0.10095
N	0.03690	0.03690
C	0.18571	0.18571
O	0.67644	0.67642
^{10}B		0.00003

heading towards the irradiation window is covered by an 0.2 cm thick 100 % enriched ^{6}LiF tile.

The diffusion length L in both mixtures for thermal neutrons will approximate the diffusion length of water which is 2.8 cm. In case of an infinite medium, over a distance of 3L from the neutron source point the thermal neutron fluence rate will decrease by a factor 20 at least. Based on this consideration, a model is constructed to calculate neutron fluence rates from the top of the tumour until 7.5 cm inside the phantom.

Like in the case of the free beam, for the construction of the cells of the model, azimuthal symmetry was asssumed.

Fig. 2.3 shows in detail the MCNP4A model and the cells, where fluence rates are calculated. Fig. 2.4 gives the positions of the cells for the tumour bearing phantom when the distance between the top of the tumour and the bismuth slab is 5 cm, the position of the bismuth slab, the D_2O moderator slab and the reactor.

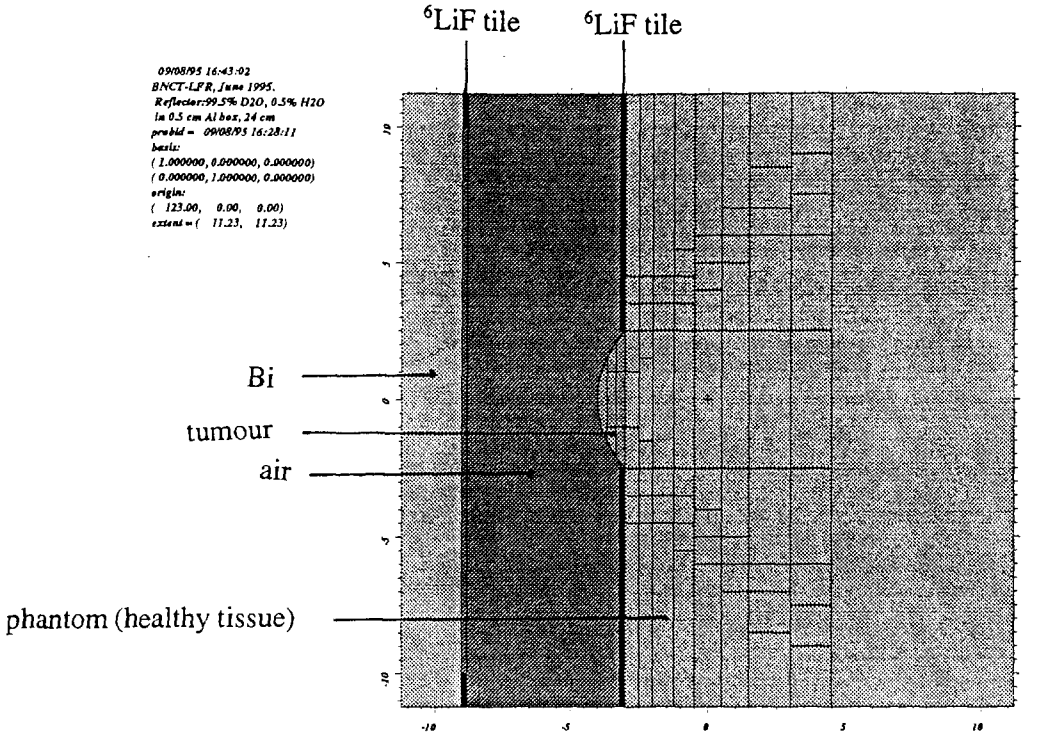

Figure 2.3 Detailed view of cells used in the MCNP4A model of the tumour bearing phantom at 5 cm from the bismuth shield.

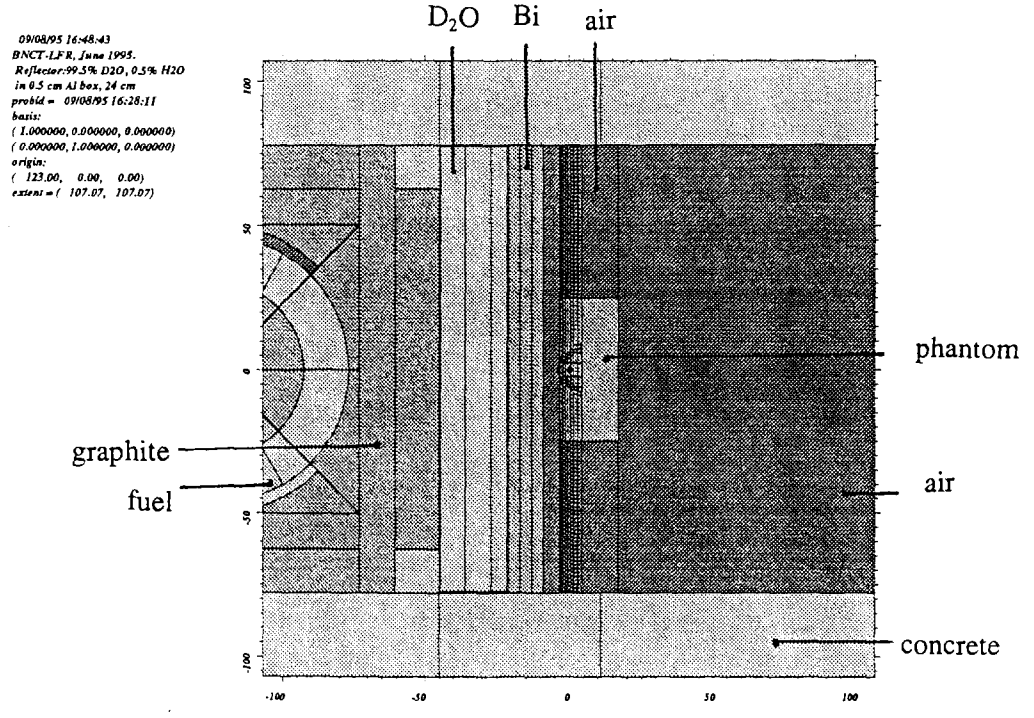

Figure 2.4 Overview of the positions of MCNP4A cells for the tumour bearing phantom, the distance between the top of the tumour and the bismuth slab being 5 cm, the bismuth slab, the D_2O moderator slab and the reactor.

3. RESULTS OF CALCULATIONS

3.1 Free beam

The thermal fluence rates (E < 0.5 eV) in the free beam are given in fig. 3.1. The results for the fluence rates of the two epithermal groups and the fast group in the free beam are given in the first appendix in fig. A.1 (0.5 eV < E < 10 keV), fig. A.2 (10 keV < E < 1MeV) and fig. A.3 (E > 1MeV), respectively.

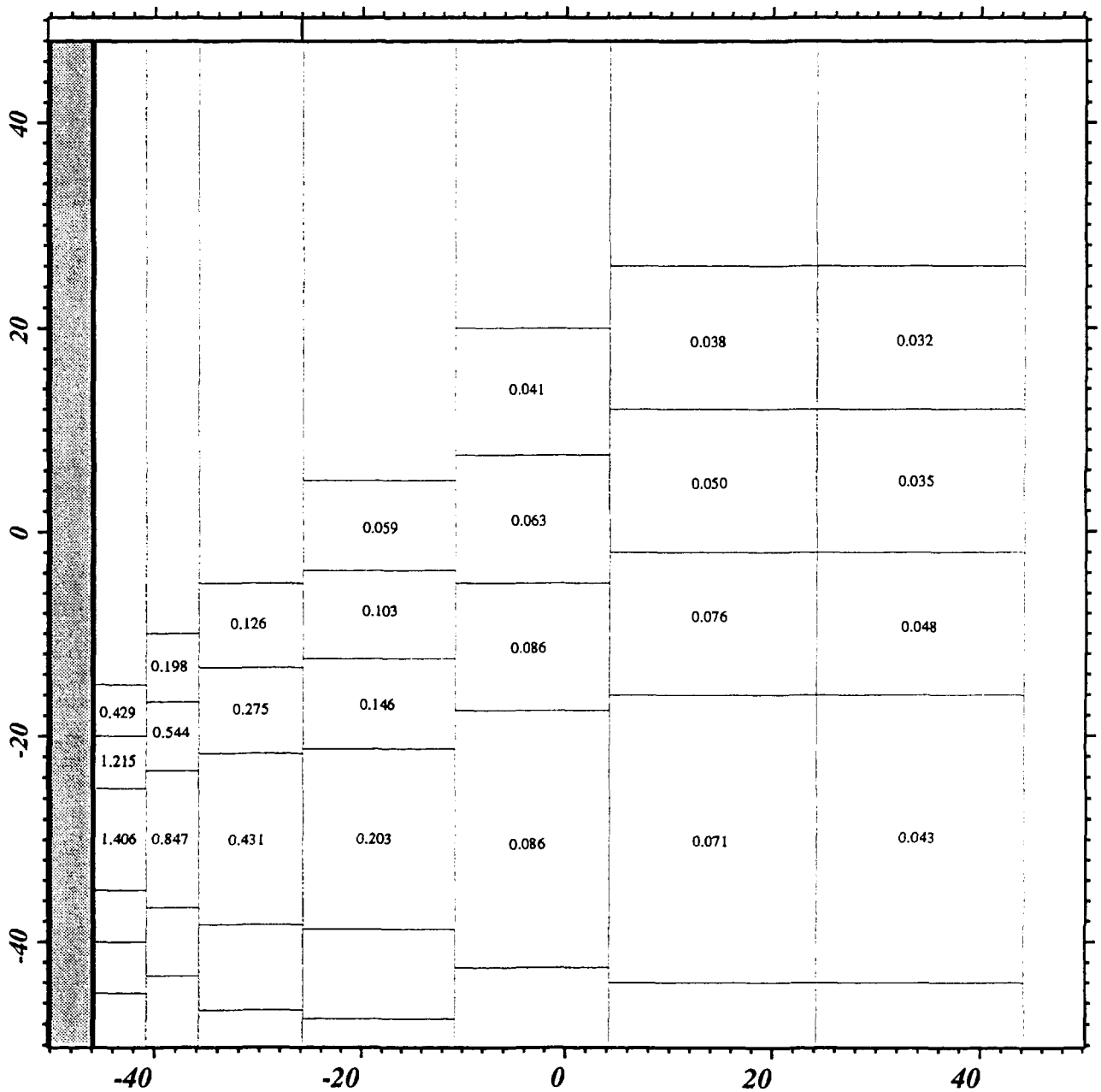

Figure 3.1 Thermal fluence rates (E < 0.5 eV) in the free beam [1.0E + 09 $cm^{-2}s^{-1}$]. From the left to the right, the standard deviations due to the Monte Carlo process are within 5 % in the first three cilinders, within 10 % in the next two and within 20 % in the last cilinder.

A histogram plot of the thermal fluence rates for the free beam is given in fig. 3.2.

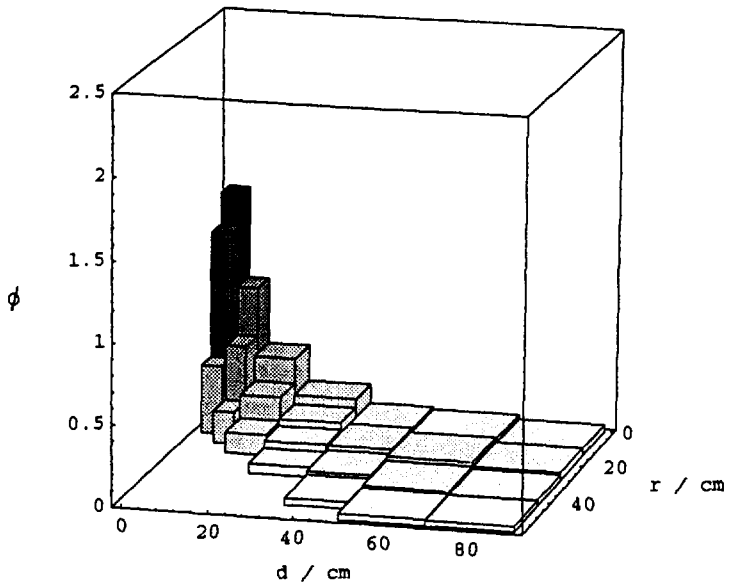

Figure 3.2 Thermal fluence rates (E < 0.5 eV) in the free beam in [1.0E + 09 $cm^{-2}s^{-1}$]; *d* denotes the distance from the Bi shield, *r* is the radial distance from the centre line of the model.

3.2 Tumour bearing phantom

The thermal fluence rates (E < 0.5 eV) in the tumour bearing phantom are given in fig. 3.3 and fig. 3.4 for a distance between the top of the tumour and the bismuth slab of 5 cm and 10 cm, respectively.

Histogram plots of the thermal fluence rates in the tumour bearing phantom for a distance between the top of the tumour and the bismuth shield of 5 cm and 10 cm are given in fig. 3.5.

The results for the fluence rates of the two epithermal groups and the fast group in the case of 5 cm distance between the top of the tumour and the LiF cover of the bismuth shield are given in the second appendix in fig. B.1 (0.5 eV < E < 10 keV), fig. B.2, (10 keV < E < 1MeV) and fig. B.3 (E > 1MeV), respectively. In case of 10 cm distance between the top of the tumour and the bismuth shield, results for the fluence rates of the two epithermal groups and the fast group are given in the third appendix in fig. C.1 (0.5 eV < E < 10 keV), fig. C.2, (10 keV < E < 1MeV) and fig. C.3 (E > 1MeV), respectively.

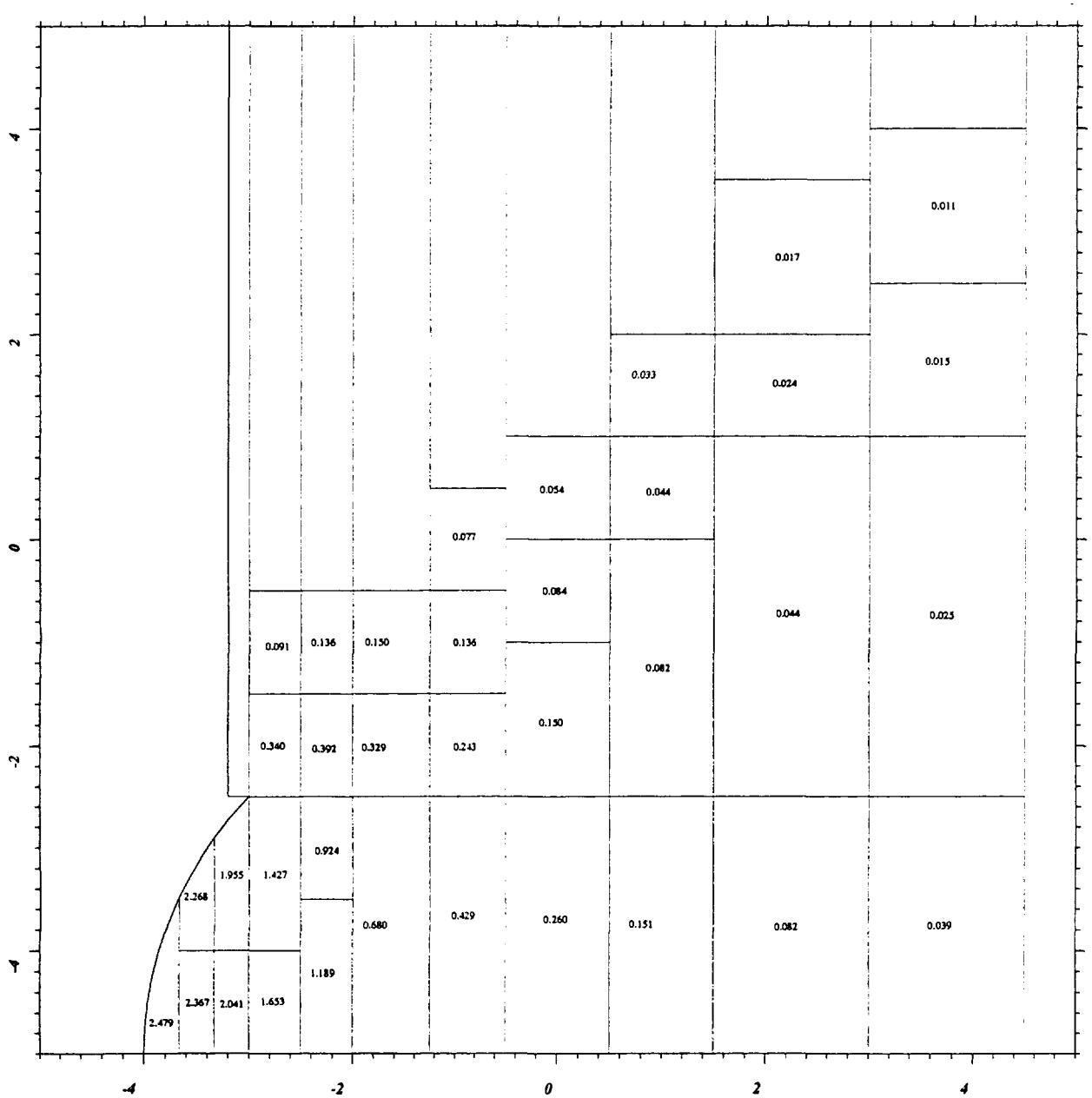

Figure 3.3 Thermal fluence rates (E < 0.5 eV) in the tumour bearing phantom for a distance between the top of the tumour and the bismuth shield of 5 cm [1.0E + 09 $cm^{-2}s^{-1}$]. All standard deviations due to the Monte Carlo process are within 5 %.

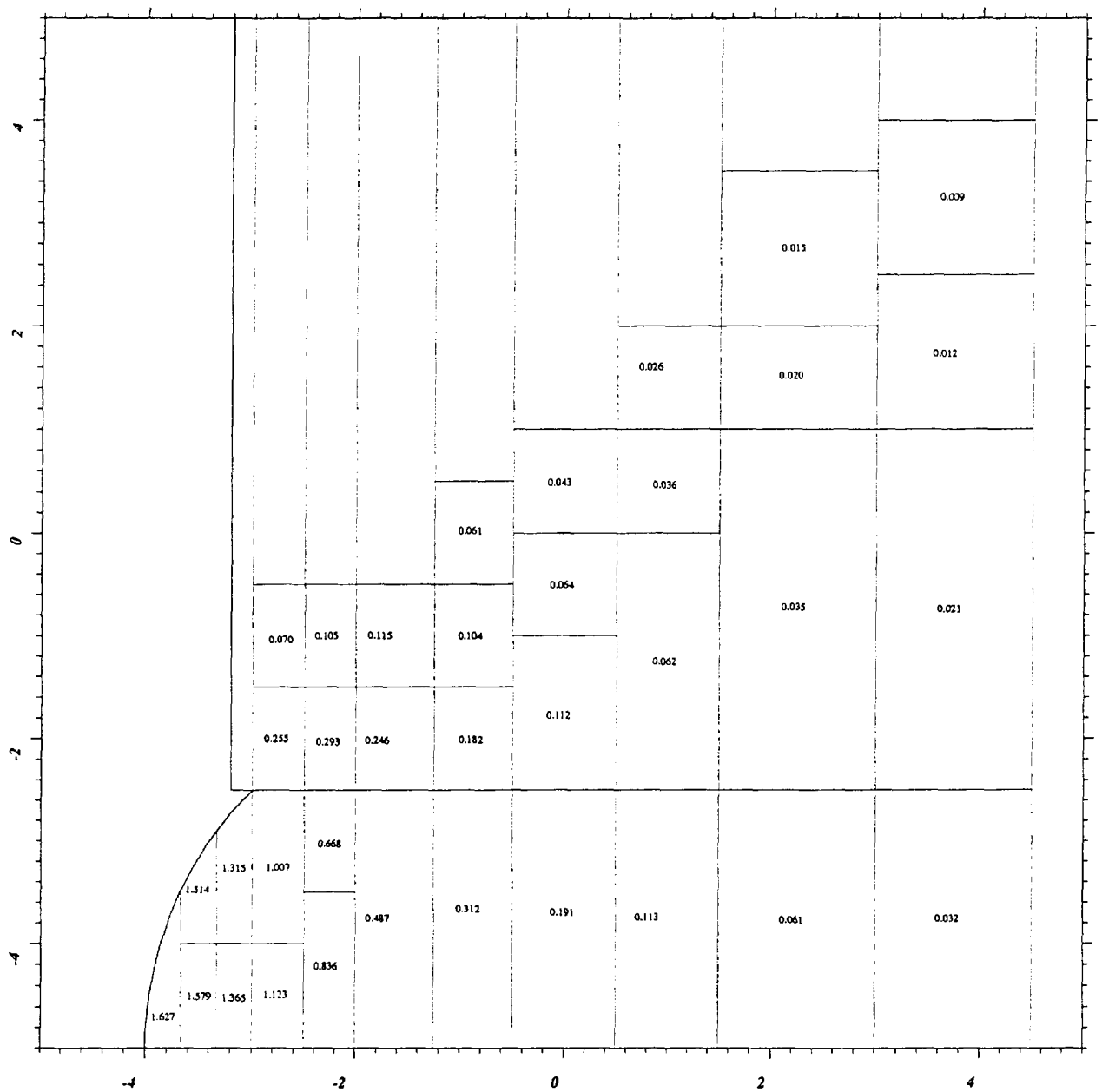

Figure 3.4 Thermal fluence rates (E < 0.5 eV) in the tumour bearing phantom for a distance between the top of the tumour and the bismuth shield of 10 cm [1.0E + 09 $cm^{-2}s^{-1}$]. All standard deviations due to the Monte Carlo process are within 5 %.

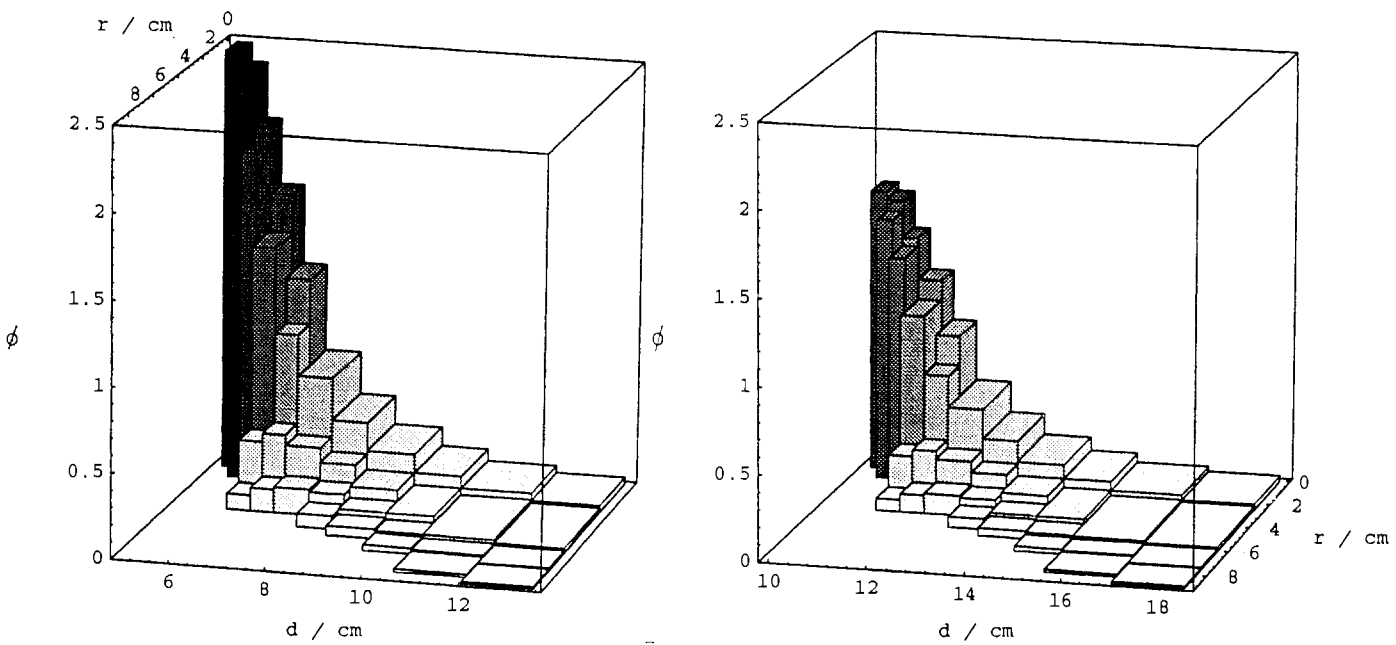

Figure 3.5 Thermal fluence rates (E < 0.5 eV) in the tumour bearing phantom in [1.0E + 09 $cm^{-2}s^{-1}$] for a distance between the top of the tumour and the bismuth shield of 5 cm (left) and 10 cm (right); *d* denotes the distance from the Bi shield, *r* is the radial distance from the centre line of the model.

4. CONCLUSIONS

- Due to thermalization and back scattering the thermal fluence rate in the superficial tumour at 5 and 10 cm distance from the bismuth shield is approximately twice as high as the thermal fluence rate in the free beam at the corresponding positions of 5 to 6 cm and 10 to 11 cm distance from the bismuth slab.
- Because the LiF cover of the bismuth only shields thermal neutrons, the fast fluence rates in the phantom are approximately constant at planes parallel to the bismuth shield.
- Due to thermalization and diffusion from the uncovered part of the phantom, the thermal fluence rate increases slightly behind the LiF cover of the healthy tissue of the phantom.
- The present study indicates the potential of the LFR as a neutron source for BNCT applied to superficial tumours, for instance of the type melanoma: The fluence rate of thermal neutrons at the surface of a tumour-phantom irradiated in the proposed clinical facility at the LFR amounts to 2.5 10^9 $cm^{-2}s^{-1}$. This is a factor of 2.5 higher than the corresponding value for the first successful clinical trial on a surface melanoma in Japan [6].

REFERENCES

[1] Peeters, T.T.J.M. and Freudenreich, W.E.: *Investigation of the possibility to use the LFR for clinical BNCT*, ECN-memo NFA-BNCT-95-01, Petten, July 1995.

[2] Freudenreich, W.E.: *Calculation of fluence rate distributions in a pre design clinical facility for BNCT at the LFR*, Schedule for Work Planning, Project Nr. 11099.03, Petten, August 21, 1995.

[3] Hogenbirk, A.: *Contents of the JEF-2.2 based neutron cross-section library for MCNP4A*, ECN-I-95-017, Petten, May 23, 1995.

[4] Briesmeister, J.G., Ed.: *MCNP - A General Monte Carlo N - Particle Transport Code*, Version 4A, LA-12625-M, Los Alamos National Laboratory, November 16, 1993.

[5] Stecher-Rasmussen, F., *private communication*, august 1995.

[6] Y. Mishima et al., *New thermal neutron capture therapy for malignant melanoma: melanogenesis-seeking ^{10}B molecule-melanoma cell interaction from in vitro to first clinical trial*, Pigment Cell Research, 1989; vol. 2, 226.

APPENDIX A. ϕ, E > 0.5 eV, free beam

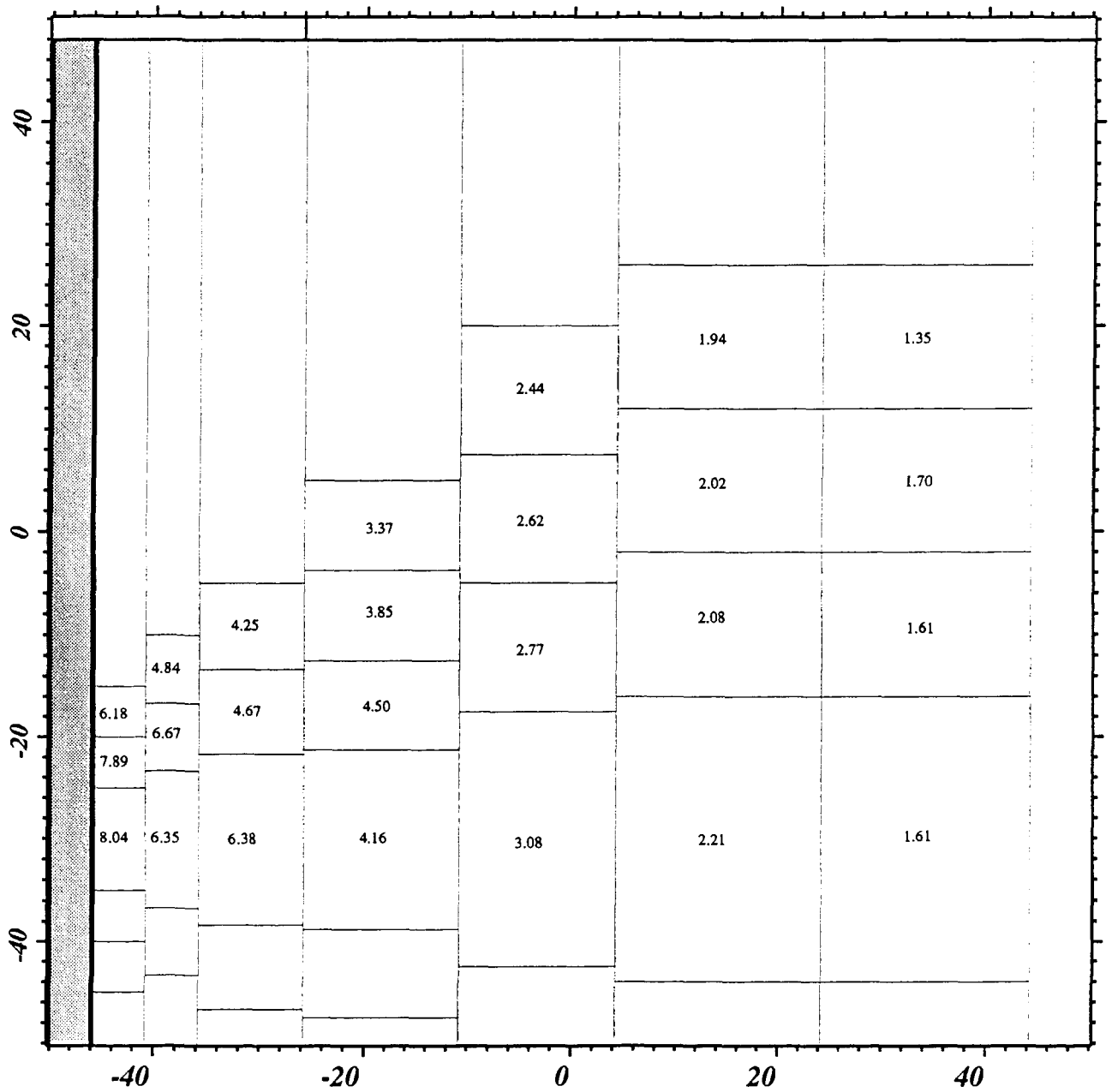

Figure A.1 Epithermal fluence rates (0.5 eV < E < 10 keV) in the free beam [1.0E + 06 $cm^{-2}s^{-1}$].
All standard deviations due to the Monte Carlo process are within 10 %.

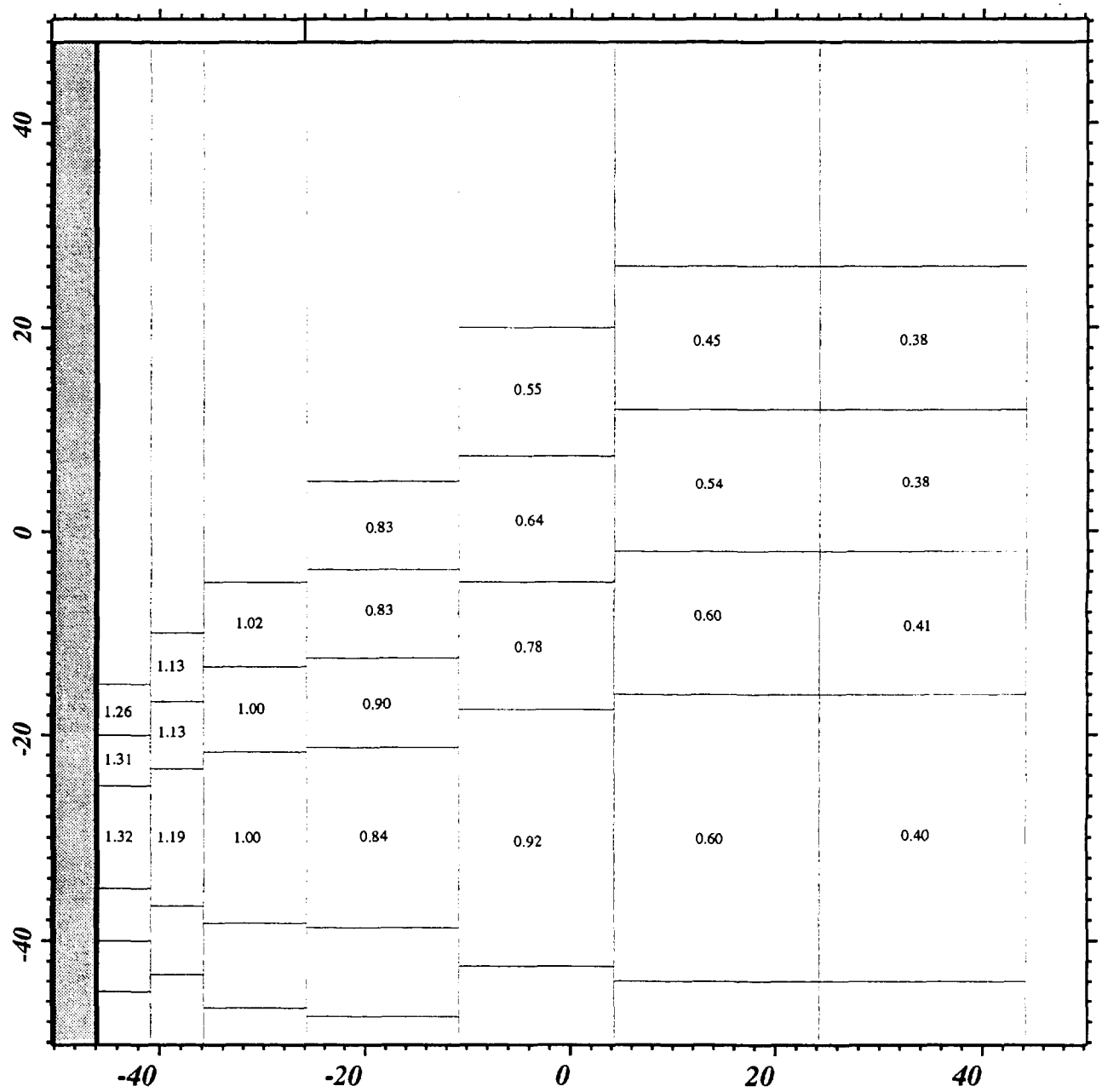

Figure A.2 Epithermal fluence rates (10 keV < E < 1MeV) in the free beam [1.0E+06 $cm^{-2}s^{-1}$]. All standard deviations due to the Monte Carlo process are within 10 % except for the central cell of the fifth cilinder left from the bismuth shield. In this case the standard deviation amounted 25 %

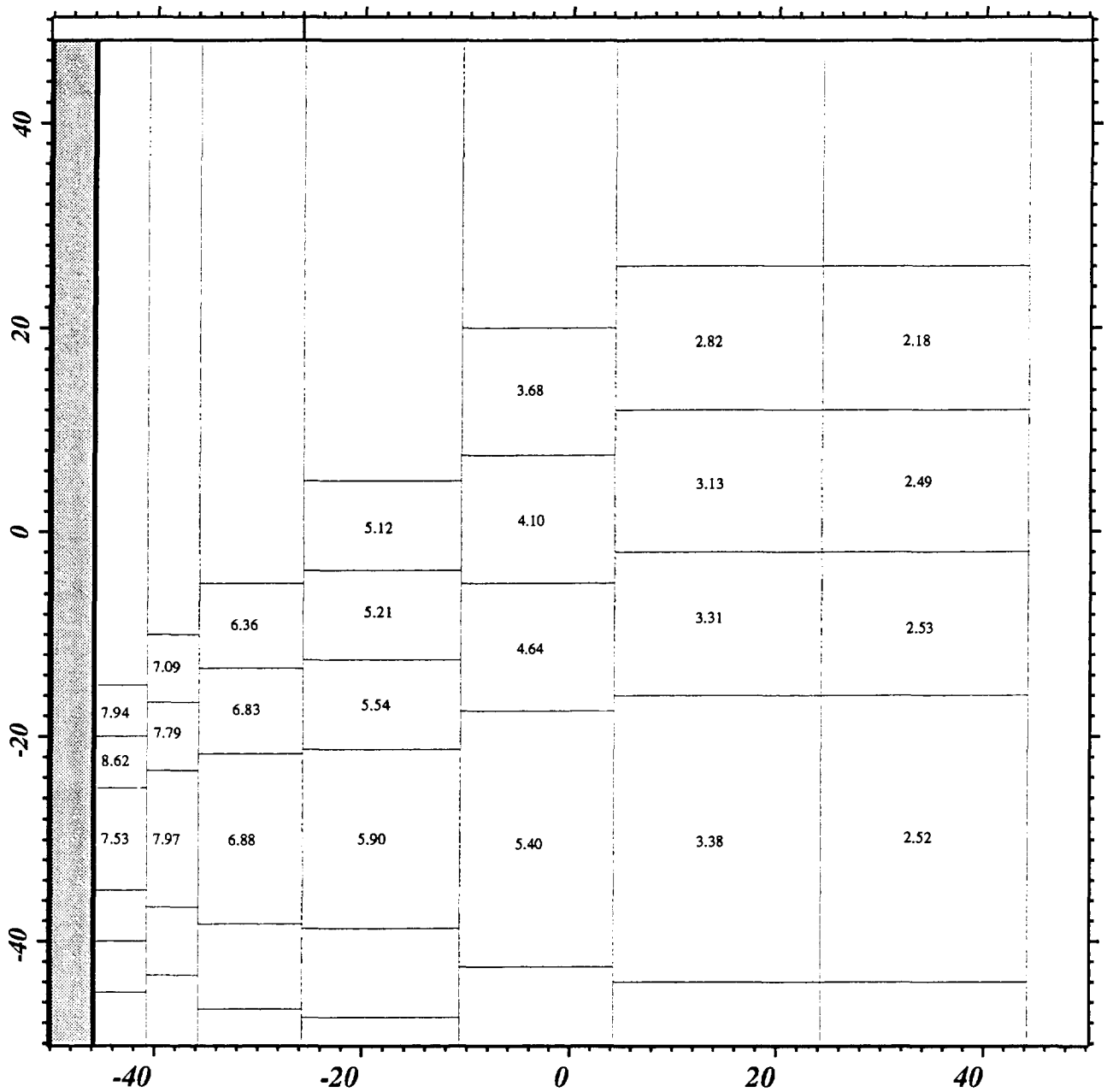

Figure A.3 Fast fluence rates (E > 1 MeV) in the free beam [1.0E + 05 $cm^{-2}s^{-1}$].
All standard deviations due to the Monte Carlo process are within 10 %.

APPENDIX B. ϕ, E > 0.5 eV, tumour at 5 cm from irradiation window

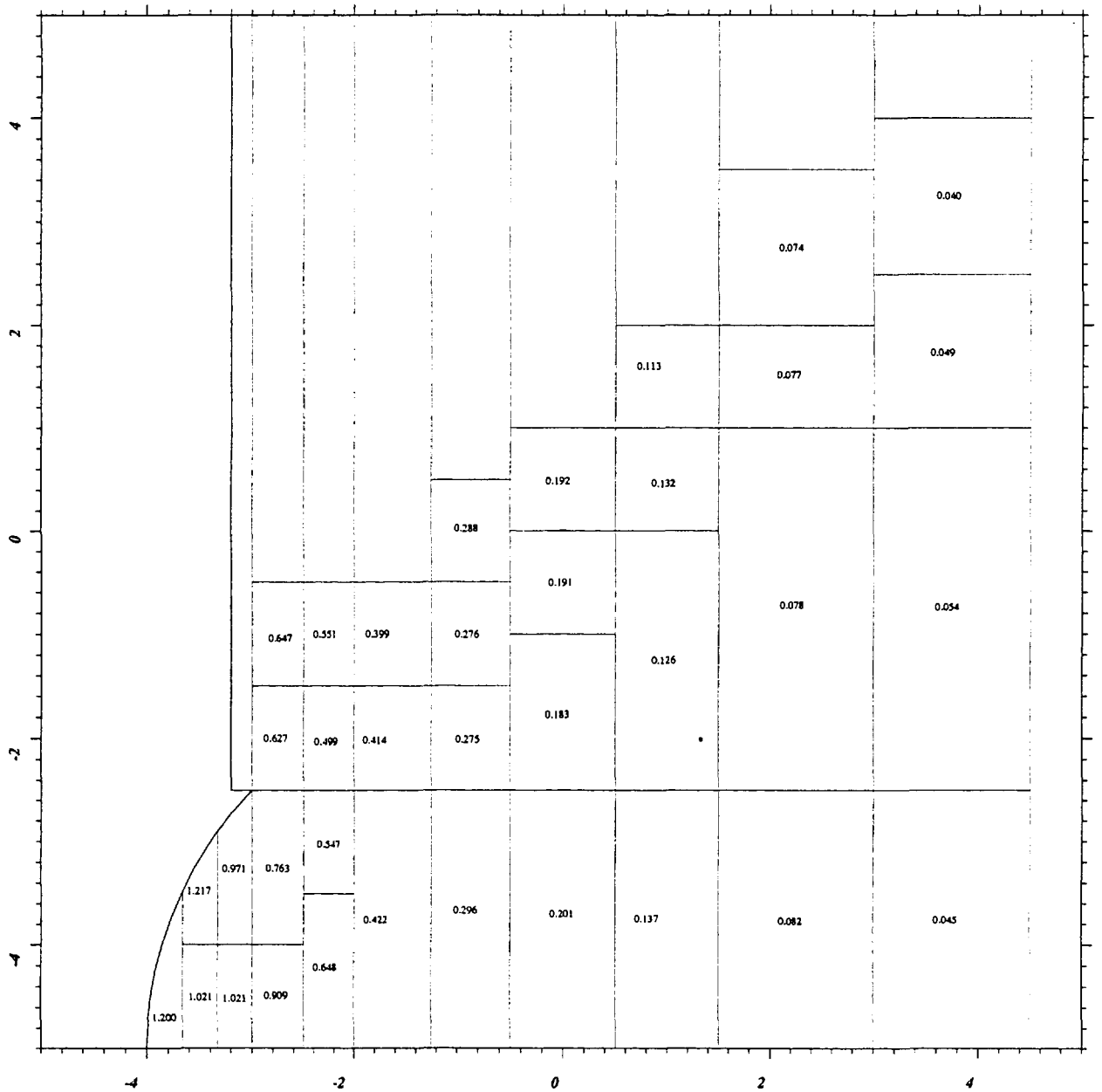

Figure B.1 Epithermal fluence rates (0.5 eV < E < 10 keV) in the tumour bearing phantom, 5 cm between top of tumour and bismuth shield [1.0E + 07 $cm^{-2}s^{-1}$]. From the left to the right, the standard deviations due to the Monte Carlo process are within 20 % in the tumour, within 15 % in the first cilinder, within 10 % in the next six and within 20 % in the last cilinder.

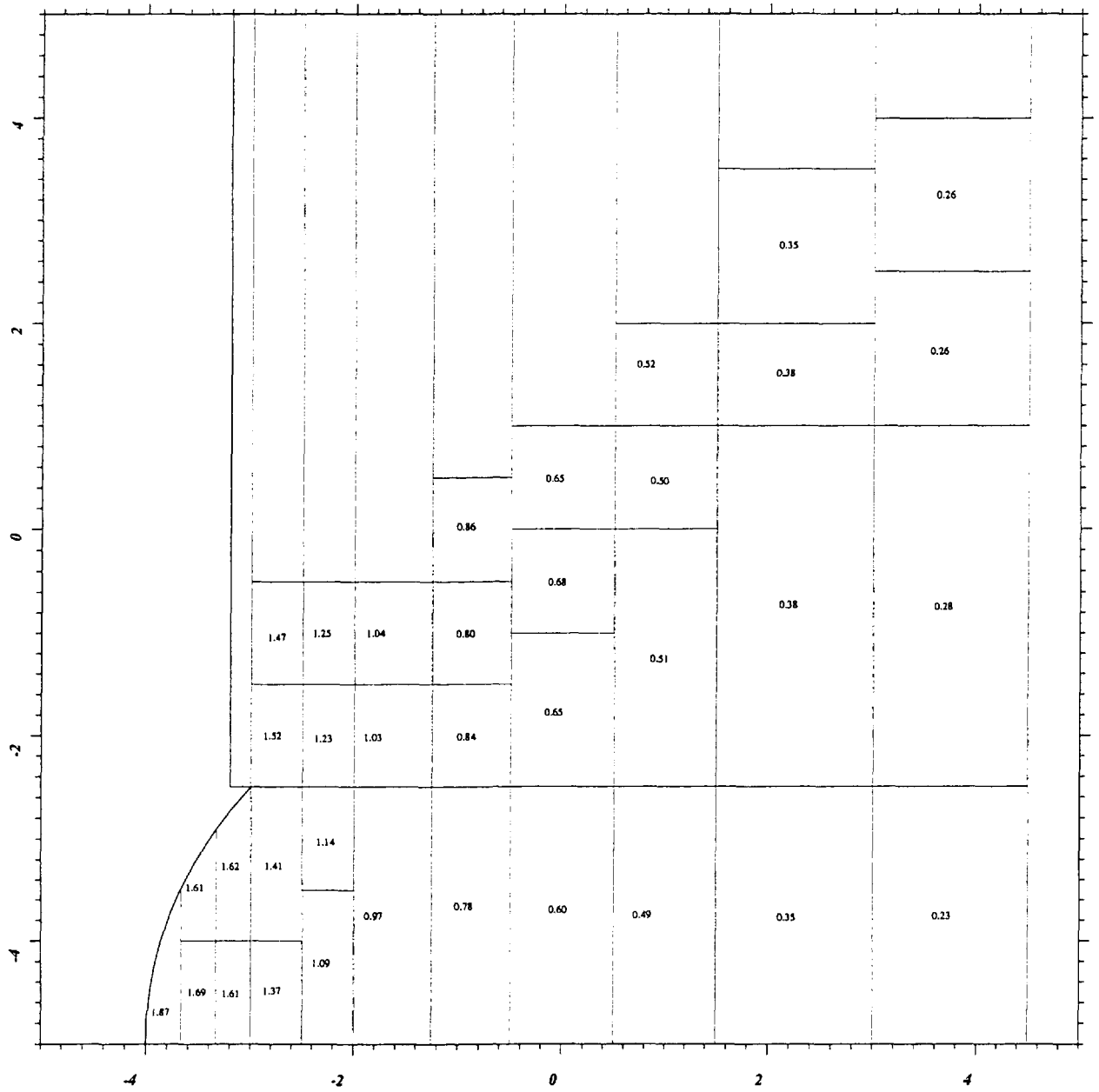

Figure B.2 Epithermal fluence rates (10 keV < E < 1MeV) in the tumour bearing phantom, 5 cm between top of tumour and bismuth shield [1.0E + 06 $cm^{-2}s^{-1}$].
From the left to the right, the standard deviations due to the Monte Carlo process are within 10 % in the tumour and the first cilinder, and within 5 % in the other seven cilinders.

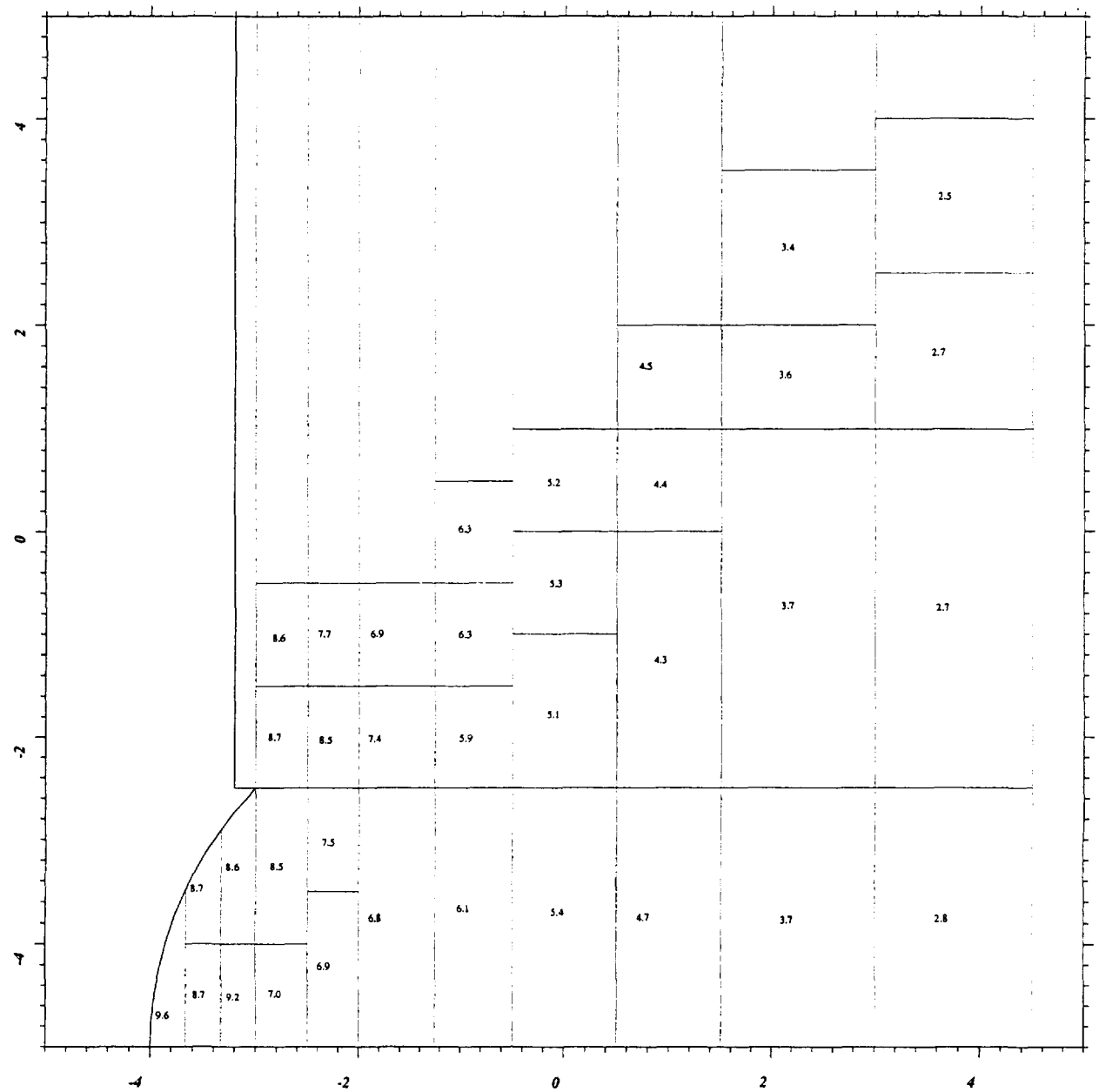

Figure B.3 Fast fluence rates (E > 1MeV) in the tumour bearing phantom, 5 cm between top of tumour and bismuth shield [1.0E + 05 $cm^{-2}s^{-1}$]. From the left to the right, the standard deviations due to the Monte Carlo process are within 20 % in the tumour, within 10 % in the next seven cilinders and within 5 % in the last cilinder.

APPENDIX C. ϕ, E > 0.5 eV, tumour at 10 cm from irradiation window

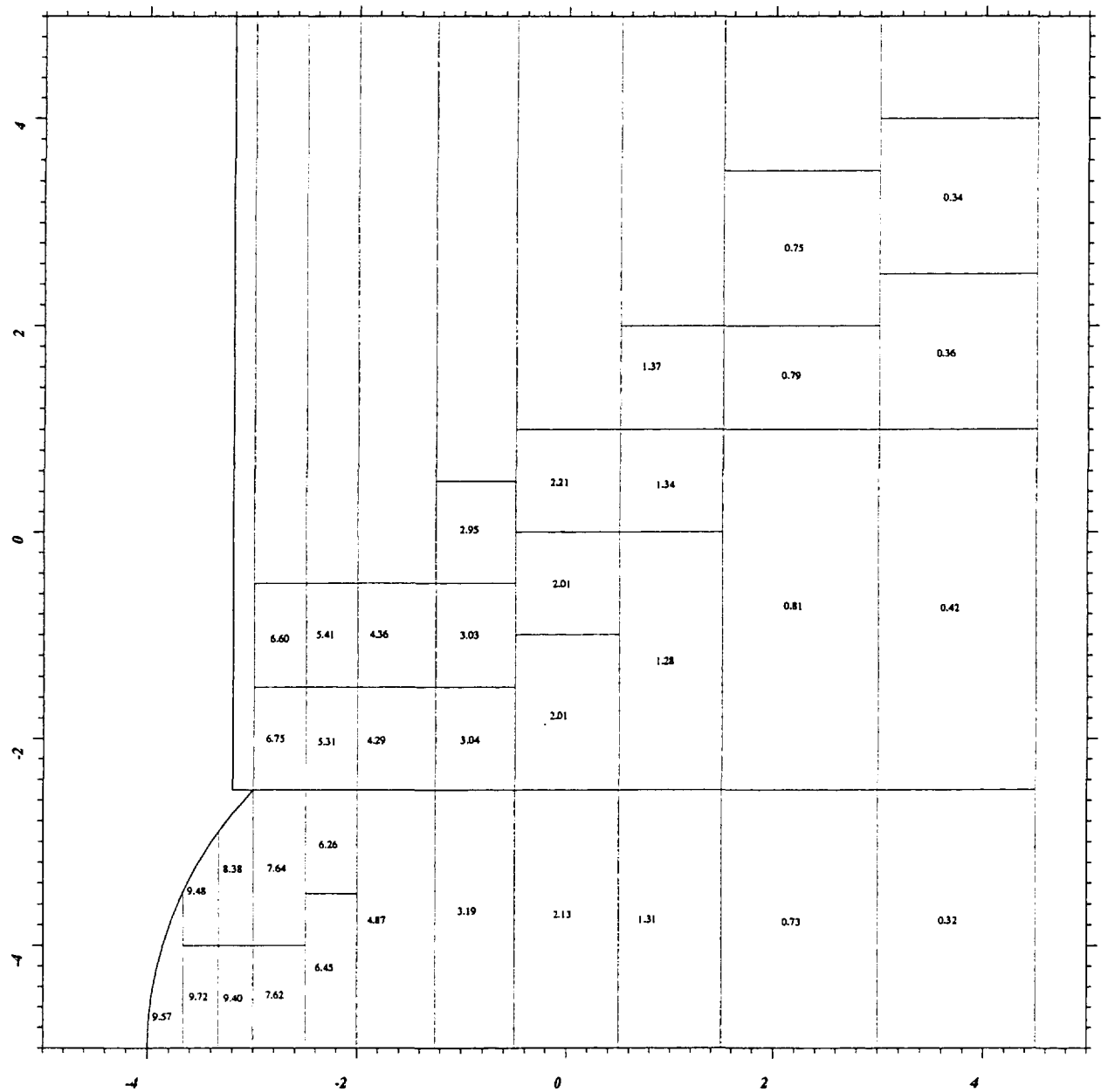

Figure C.1 Epithermal fluence rates (0.5 eV < E < 10 keV) in the tumour bearing phantom, 10 cm between top of tumour and bismuth shield [1.0E + 06 $cm^{-2}s^{-1}$].
From the left to the right, the standard deviations due to the Monte Carlo process are within 20 % in the tumour, within 10 % in the next seven cilinders and within 15 % in the last cilinder.

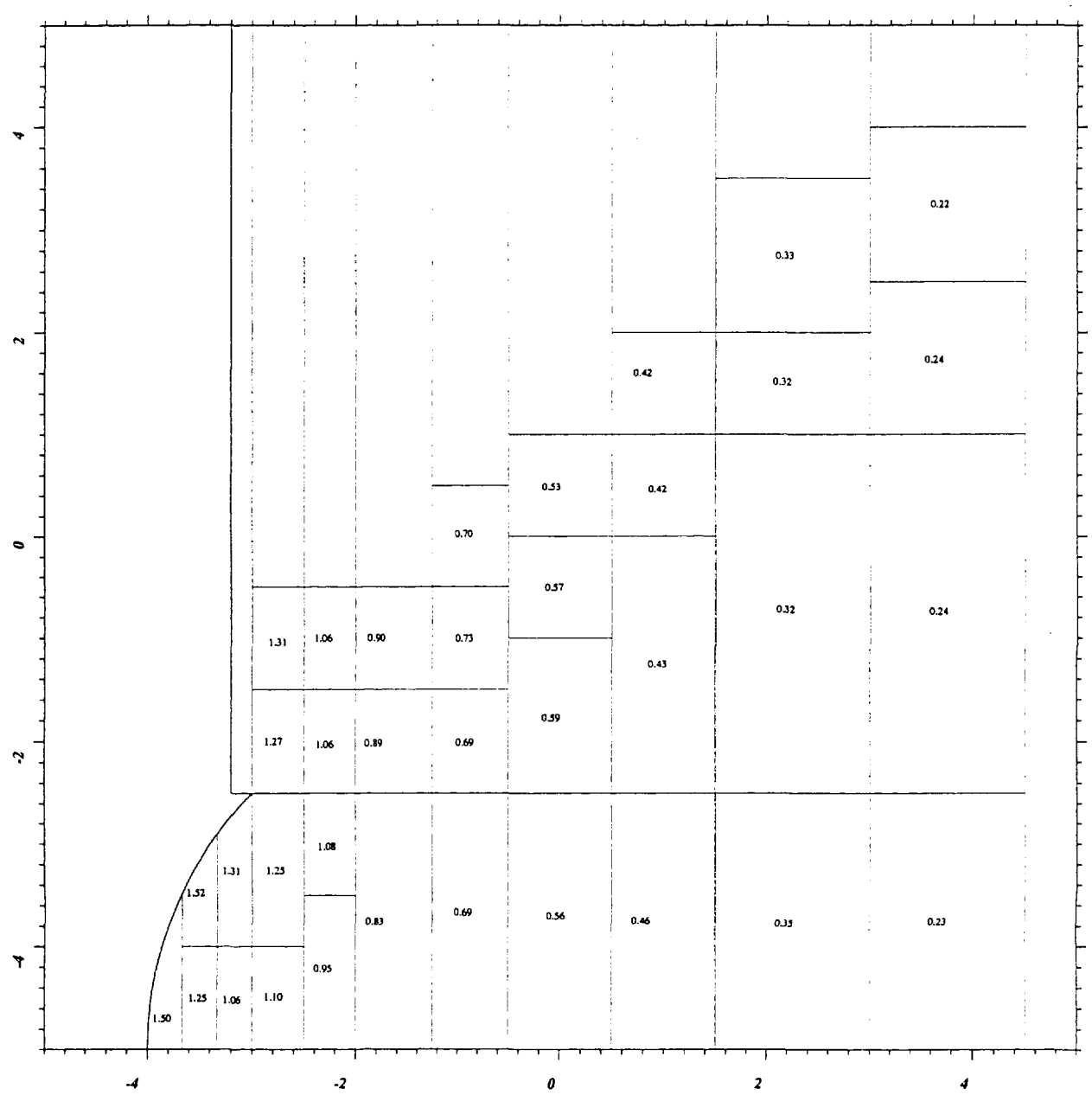

Figure C.2 Epithermal fluence rates (10 keV < E < 1 MeV) in the tumour bearing phantom, 10 cm between top of tumour and bismuth shield [1.0E + 06 $cm^{-2}s^{-1}$]. From the left to the right, the standard deviations due to the Monte Carlo process are within 15 % in the tumour and within 5 % in the other cilinders.

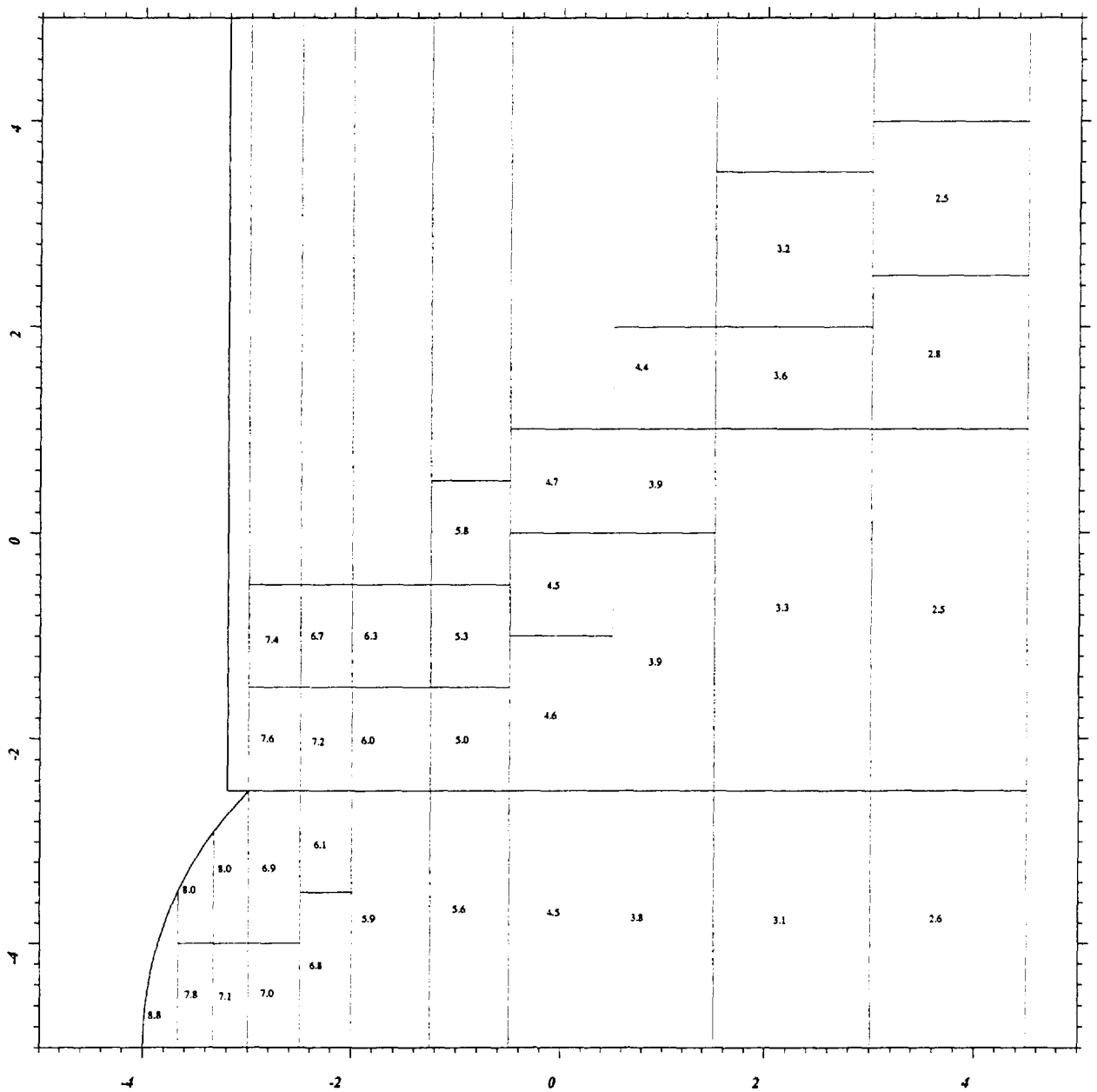

Figure C.3 Fast fluence rates (E > 1MeV) in the tumour bearing phantom, 10 cm between top of tumour and bismuth shield [1.0E + 05 $cm^{-2}s^{-1}$].
From the left to the right, the standard deviations due to the Monte Carlo process are within 20 % in the tumour and within 10 % in the other cilinders.